Atmos. Chem. Phys. Discuss., 9, 5263–5287, 2009
www.atmos-chem-phys-discuss.net/9/5263/2009/

Atmospheric Chemistry and Physics Discussions

This discussion paper is/has been under review for the journal *Atmospheric Chemistry and Physics (ACP)*. Please refer to the corresponding final paper in *ACP* if available.

Effects of boundary layer particle formation on cloud droplet number and changes in cloud albedo from 1850 to 2000

J. Merikanto[1], **D. V. Spracklen**[1], **K. J. Pringle**[2], **and K. S. Carslaw**[1]

[1]School of Earth and Environment, University of Leeds, Leeds, UK
[2]Max Planck Institute for Chemistry, Mainz, Germany

Received: 21 October 2008 – Accepted: 23 January 2009 – Published: 27 February 2009

Correspondence to: J. Merikanto (j.merikanto@leeds.ac.uk)

Published by Copernicus Publications on behalf of the European Geosciences Union.

Abstract

We use a global aerosol microphysics model to estimate the effect of boundary layer particle formation on cloud droplet number concentration (CDNC) on global and regional scales. The calculations are carried out for years 1850 and 2000 using historical emissions inventories for primary particles and aerosol precursor gases. Predicted CDNC in 2000 are in good agreement with in-situ observations when particle formation is included. We find that particle formation increases global annual mean CDNC by approximately the same amount in both years (16.0% in 1850 and 13.5% in 2000). Thus, global mean changes in cloud albedo are similar with and without particle formation. However, there are substantial regional effects of up to 50% enhancement or suppression of the 1850–2000 albedo change. Over most modern-day polluted Northern Hemisphere regions particle formation suppresses the 1850–2000 increase in CDNC and cloud albedo. Over the Arctic the albedo change is suppressed by 23% in the annual mean and by 43% in summer when particle formation is taken into account. The albedo change of the persistent stratocumulus cloud deck west of Chile is enhanced by 49%.

1 Introduction

Cloud droplet number concentration (CDNC) is controlled by the concentration of aerosol particles large enough to act as cloud condensation nuclei (CCN) (Lohman and Feichter, 2005; Dusek et al., 2006). The CDNC depends on the concentration, size distribution and chemical properties of CCN and on the updraft velocity defining the maximum supersaturation in a cloud parcel (Nenes and Seinfeld, 2003). Higher CDNC leads to an enhanced cloud albedo (Twomey, 1991). This effect is known as the first indirect effect, and its magnitude is one of the most poorly quantified factors in assessing human impacts on climate (IPCC, 2007). Estimates of the aerosol indirect effect obtained from different global climate models (GCMs) vary from $-0.3\,W/m^2$ to $-1.8\,W/m^2$,

ACPD

9, 5263–5287, 2009

and the main cause of the spread in results is the difference in predicted aerosol concentrations between different models given a fixed set of sources (Penner et al., 2006).

Observations from several locations around the world suggest that formation of new aerosol particles by nucleation is a frequent phenomenon (Kulmala et al., 2004a). These particles can be first detected in the 3–10 nm diameter range, and their subsequent growth to CCN sizes can be followed. Locally, particle formation has been observed to contribute significantly to CCN (Lihavainen et al., 2005; Kerminen et al., 2005; Laaksonen et al., 2005). Although the fundamental formation mechanism of secondary particles is not well understood, extensive observations in the atmospheric boundary layer (BL) show that the rate of new particle formation is proportional to the sulfuric acid concentration to power 1 or 2 (Weber et al., 1995, 1997; Sihto et al., 2006; Riipinen et al., 2007; Kuang et al., 2008). Measurements also indicate that the main growth mechanics of the newly formed particles is the condensation of secondary organics together with sulfuric acid (O'Dowd et al., 2002). A different mechanism appears to occur above the boundary layer (BL), which is often represented in models as binary homogeneous nucleation of sulfuric acid-water particles (Kulmala et al., 1998; Spracklen et al., 2005, 2006; Adams and Seinfeld, 2002).

In a previous study we used a global aerosol microphysics model to demonstrate that particle formation in the BL increases the global mean CCN (0.2% supersaturation) concentrations by 3–20% and CCN (1%) by 5–50% (Spracklen et al., 2008). The uncertainties in these values are related to uncertainties in particle formation and growth rates. Thus particle formation is an important, though still quite uncertain, source of CCN in the present atmosphere. But the important question for climate is whether the contribution of particle formation to CCN has changed over the industrial period, which would affect the calculated aerosol indirect forcing. There are reasons to suspect that it might have changed. In Spracklen et al. (2006) we showed that changes in primary emissions could lead to non-linear changes in particle number: primary emissions are a source of particles but also a sink for nuclei. We showed that the total number of particles initially goes down as primary emissions are reduced, but as they are reduced

ACPD
9, 5263–5287, 2009

further particle number goes up again because particle formation becomes enhanced. Gaydos et al. (2005) and Jung et al. (2006) also showed a non-linear response of nucleation to SO_2 emissions in a box model. But the impact of long-term changes in nucleating vapours and primary particles is likely to be complex and regionally variable because of the non-linear response of nucleation to production and loss processes.

Here, we extend our model simulations of present day CCN to quantify the effect of boundary layer particle formation on CDNC and cloud albedo under pre-industrial (1850) and present-day (2000) conditions. We use a mid-range estimate for the particle formation rate leading to a 10–20% increase in global present-day CCN. Our aim is not to calculate a new value for the indirect forcing, but to demonstrate that while work is in progress to improve the representation of aerosol in GCMs, particle formation should be considered due to its sizable contribution to CDNC and to estimates of the cloud albedo change.

2 Model description

We use the global aerosol microphysics model GLOMAP, which is an extension of the offline 3-D chemical transport model TOMCAT (Chipperfield, 2006). Full details of the model microphysics scheme are described in Spracklen et al. (2005). GLOMAP treats two externally mixed aerosol distributions described by a two-moment sectional scheme with 20 sections spanning 3 nm to 25 μm dry diameter. One of the distributions is partly hydrophyllic including sulfate, sea-salt, black carbon (BC) and organic carbon (OC). The other distribution representing freshly emitted primary carbonaceous particles contains BC and OC and is assumed to be hydrophobic. The hydrophobic OC and BC particles are transferred to the hydrophyllic distribution through coagulation and condensation of soluble gas-phase species. These species include gaseous H_2SO_4 and the first-stage oxidation products of monoterpenes (Guenther et al., 1995), which form hydrophilic secondary organic aerosol material with an assumed yield of 13%. The model has a horizontal resolution of ~2.8° by ~2.8° with 31 vertical levels

ACPD
9, 5263–5287, 2009

between the surface and 10 hPa and is forced by analyses from the European Centre for Medium-Range Weather Forecasts for the year 2000. The same meteorology and oxidants are used both for 1850 and 2000 runs.

New particle formation is modelled with the cluster activation theory (Kulmala et al., 2006). The particle formation rate with this scheme can be described by

$$J_1 = A[H_2SO_4], \quad (1)$$

where J_1 is the production rate of 1 nm clusters, $[H_2SO_4]$ is the gas phase sulfuric acid concentration in cm^{-3} and A is the activation coefficient. Here we have used $A=2\times10^{-6}\,s^{-1}$, which is based on empirical calculations (Sihto et al., 2006) and on our previous comparisons with ground level observations (Spracklen et al., 2006, 2008). The effective production rate of 3 nm particles added to the first size bin is obtained with the parameterization of Kerminen and Kulmala (2002), expressed as

$$J_3 = J_1 \exp\left(-0.153\frac{CS'}{GR}\right), \quad (2)$$

where CS′ is the reduced condensation sink and GR ($nm\,h^{-1}$) is the cluster growth rate, assumed to be constant between 1 nm and 3 nm and given by $0.73\times10^{-7}[H_2SO_4]$. In reality, the growth rate may depend on the concentration of secondary organics and on the particle size (Kulmala et al., 2004b; Hirsikko et al., 2005). However, a large body of experimental evidence supports the idea that particle formation rates depend mainly on the interplay between the sulfuric acid concentration and condensation sink, as in the above parameterization.

The above particle formation mechanism is confined to the BL in our model runs. Aircraft observations suggest that the total particle concentration has a minimum just above the BL (Schroder, 2002). The concentrations increase again in the free and upper troposphere, where homogeneous binary H_2O-H_2SO_4 or ternary H_2O-H_2SO_4-NH_3 particle formation mechanisms are the most likely sources of new particles (see e.g. Kulmala et al., 1998; Merikanto et al., 2007). Above the boundary layer we use

ACPD
9, 5263–5287, 2009

the parameterized H_2O-H_2SO_4 particle formation rates of Kulmala et al. (1998), which we have previously shown to reproduce the observed particle number concentrations in the upper troposphere (Spracklen et al., 2005). However, in this study we focus only on the effects of BL particle formation.

The cloud drop number concentration (CDNC) is calculated from the time-averaged hydrophyllic particle distribution using the iterative scheme of Nenes and Seinfeld (2003) and Fountoukis and Nenes (2005). The schemes take into account the fraction of soluble material in the particles and the number of ions released into the solution, and are capable of predicting the observed CDNC with good accuracy (Meskhidze et al., 2005). The calculations are carried out for every grid box regardless of the presence of clouds at 300–1000 m above ground level. The CDNC are calculated as a diagnostic and are not fed back into the aerosol microphysics.

The changes in aerosol, and hence in cloud drop number, are quantified using emissions for 1850 and 2000. The anthropogenic sulfur emissions, accounting also for changes in wildfires, are taken from the inventory of Smith et al. (2004). According to this inventory, the global sulfur emissions have increased from 1.4 to 59.4 TgS/yr between 1850 and 2000. We emit 2.5% of sulfur directly as particulate sulfate with mode diameters of 60 nm (50% of ground level sulfate emissions), 150 nm (50% of ground level sulfate emissions), 150 nm (50% of elevated sulfate emissions) and 1500 nm (50% of elevated sulfate emissions). The remaining 97.5% of athropogenic sulfur is emitted as SO_2. The marine dimethylsulfide emissions and sulfur emissions from constantly erupting volcanoes are assumed to be the same for both years, accounting for 17.7 TgS/yr and 13.0 TgS/yr, respectively. We use the inventory of Bond et al. (2007) for energy related emissions of BC and OC, and further separate these emissions into biofuel and fossil fuel components using the database of Fernandes et al. (2007). Monthly wildfire BC and OC emissions are from Dentener et al. (2006), where the values for 1850 are obtained by taking a population weighted average of 1750 and 2000 emissions. The total global BC particulate emissions are 2.1 Tg/yr and 8.0 Tg/yr for 1850 and 2000, respectively, and 20.5 Tg/yr and 49.2 Tg/yr for OC. The

ACPD
9, 5263–5287, 2009

sea-salt emissions are taken from Gong (2003) for both years.

3 Results

3.1 Evaluation of model cloud droplet number

As a basic check on model-predicted CDNC we have compared our results against in-situ observations from four aircraft measurement campaigns carried out over the Arctic ocean and in US (Gultepe and Isaac, 2002, 2004; Meskhidze et al., 2005; Fountoukis et al., 2007) (Table 1). The updraft velocities $\overline{w}$ during the aircraft measurements have been ecorded for each of these campaings. In our calculations we have used a representative average values of $\overline{w}$ corresponding to in-situ measurements. The CDNC values with particle formation are in good agreement with observations while the model without BL particle formation underestimates the mean CDNC in all cases. Given the uncertainties in updraft velocity, particle composition and size distribution these differences cannot be used to demonstrate that the particle formation model is correct, but overall the model-observation agreement gives confidence in predicted CDNC for present-day conditions.

3.2 Changes in aerosol and condensation sink

The formation rate of 3 nm particles depends primarily on the sulfuric acid concentration and the magnitude of the condensation sink. Figure 1 shows the ratio of 1850 and 2000 yearly mean condensation sinks and the ratio of sulfuric acid concentrations, and the concentrations of 3–10 nm particles resulting from boundary layer particle formation. Already in the relatively clean atmosphere in 1850 particle formation has produced significant amounts of new particles. Considering that the anthropogenic sulfur emissions in 1850 are only 1.4 TgS/yr compared to 30.7 TgS/yr from natural sulfur emissions most of the formation in 1850 must be driven by natural sulfur sources.

ACPD
9, 5263–5287, 2009

The gaseous sulfuric acid concentration has increased from 1850 to 2000 only over continental regions where anthropogenic emissions have increased from 1850 to 2000. Over the continents typical changes in condensation sink are smaller in magnitude than the changes in sulfuric acid concentration. Therefore, the average continental particle formation rates are larger in 2000 than in 1850. On the other hand, in many marine regions especially in the Northern Hemisphere, the condensation sink has grown due to the outflow of aged particles causing the formation rates in these regions to decrease or to stay constant. Since the condensation sink represents the effective coagulation sink for the smallest particles, a smaller portion of the newly formed marine particles is able to grow to large sizes in 2000 than in 1850.

3.3 Changes in cloud droplet number

Figure 2 shows the predicted CDNC for 1850 and 2000 with boundary layer particle formation. Here, we have used a typical value of 0.4 m/s for the cloud updraft velocity. The increase in anthropogenic emissions from 1850 to 2000 has clearly had a profound effect on the CDNC. In both 1850 and 2000 particle formation increases CDNC substantially, as shown in the lower panels of Fig. 1. Surprisingly, the globally averaged contribution of particle formation to CDNC has been quite similar in both years regardless of changes in emissions. Particle formation increases global mean CDNC by 16.0% in 1850 and 13.5% in 2000, indicating that the global contribution to CDNC has been quite similar. In both years CDNC is higher over continents than marine areas, but the marine-continent contrast is much larger in 2000 than in 1850. Large differences in continental CDNC can also be seen in less industrialized regions, like over the equatorial Africa and South America. These differences are mostly due to increases in particulate emissions from biofuel and forest burning. However, particle formation still accounts for a significant proportion of CDNC in these areas regardless that the in-situ particle formation rates are negligible. This can be seen by comparing the lower panels of Fig. 2 to the original locations of particle formation shown in the lower panels of Fig. 1. The differences in the patterns in these figures are due to

ACPD
9, 5263–5287, 2009

long range transport of particles: the effect of particle formation on CDNC spreads to remote regions where particle formation does not take place in-situ.

Changes in CDNC are summarized in Table 2 for several continental regions and marine regions with persistent stratiform cloud formation, indicated in Fig. 2. A clear increase in CDNC can be seen in all cases when particle formation is included. The globally averaged fractional changes in CDNC are quite similar in the runs with and without particle formation (66.1% and 68.7% respectively, see Table 2). However, there are large regional differences in the relative importance of particle formation. Particularly, in many parts of the Northern Hemisphere the relative contribution of particle formation in 2000 is less than in 1850. This is particularly the case in modern-day polluted regions. On the other hand, in the Southern Hemisphere the relative contribution of particle formation to CDNC is greater in 2000 than 1850. It appears that already in 1850 particle formation made a substantial contribution to Arctic CDNC both through particle transport and in-situ formation. In the Arctic, particle formation suppresses the 1850–2000 chance in CDNC. Overall, the changes in the relative importance of particle formation to CDNC show a very different pattern than the changes in CDNC if particle formation is omitted.

3.4 Changes in cloud albedo

The change in cloud albedo during the period is related to the relative change in cloud droplet number. If we assume that there have been no significant changes in the cloud liquid water content or height we can write (Twomey, 1991)

$$\Delta \mathrm{Rc} = \mathrm{Rc}(1 - \mathrm{Rc})/3 \ln\left(\frac{\mathrm{CDNC}(2000)}{\mathrm{CDNC}(1850)}\right), \quad (3)$$

where Rc is the initial albedo. The difference in cloud albedo change with and without particle formation is given by

$$d\Delta \mathrm{Rc} = \Delta \mathrm{Rc} - \Delta \mathrm{Rc}'$$

$$= \mathrm{Rc}(1-\mathrm{Rc})/3 \ln \left(\frac{\left(\frac{\mathrm{CDNC}(2000)}{\mathrm{CDNC}(1850)}\right)}{\left(\frac{\mathrm{CDNC}'(2000)}{\mathrm{CDNC}'(1850)}\right)} \right), \quad (4)$$

where the primed values indicate results without boundary layer particle formation. The logarithmic term in the above equation, the ratio of CDNC ratios between runs with and without particle formation, shows that particle formation has an effect on albedo change only if its relative contribution to CDNC has changed over time. A schematic representation of the effects of particle formation is shown in Fig. 3. It shows that particle formation can both enhance and suppress the obtained albedo changes. To calculate ΔRc we assume an initial albedo of 0.35. Although the 1850–2000 changes in albedo are affected by the assumed initial albedo, the assumption does not alter the calculated relative impact of particle formation.

Figure 4 shows the resulting changes in ΔRc with and without boundary layer particle formation. The figure shows the averaged full year and Northern Hemisphere summer values. The regional patterns of ΔRc are quite strongly affected by particle formation. For example, during the Northern Hemisphere summer particle formation completely removes the obtained albedo change over large parts of the Arctic region. The full year regional changes are summarized in Table 2. The global mean albedo change is predicted to be 3.97% with particle formation and 3.85% without, so the globally averaged impact of particle formation is negligible.

Figure 5 shows the impact of including particle formation in the model on the 2000/1850 ΔRc for four Northern Hemisphere seasons. The impact on ΔRc is given by $d\Delta\mathrm{Rc}/\mid\Delta\mathrm{Rc}'\mid$ and is independent of the initial albedo. We note that the results are similar with different updraft velocities, although the regional differences are more pronounced with higher updrafts. Blue areas in Fig. 5 indicate regions where the 1850 to 2000 changes in CDNC or ΔRc are reduced by including particle formation, and red areas indicate where the changes are increased. It can be seen that boundary layer particle formation has a substantial regional impact on calculated ΔRc. In large parts

ACPD
9, 5263–5287, 2009

of the globe $d\Delta Rc/\mid \Delta Rc' \mid$ exceeds 50%. The results show a large North-South contrast: particle formation reduces the calculated albedo change in the north and increases it in the south. Results show relatively high seasonal variation, and the largest regional changes are obtained during the Northern Hemisphere summer. During the summer the positive albedo change in the Northern Hemisphere is greatly reduced, except in North America where particle formation results in a larger positive albedo change. In the south tropics particle formation enhances the obtained albedo change during all seasons. The changes in the Antarctic region are not statistically significant since the obtained albedo change is negligible in all cases.

These model simulations show that boundary layer particle formation has a regionally variable impact on CDNC and albedo changes between 1850 and 2000. In some regions the increases in albedo are enhanced when particle formation is included, while in other regions it is suppressed. The regional differences arise because of the relative contribution of particle formation to aerosol in 1850 and 2000 has changed (illustration in Fig. 3). In regions where albedo changes are suppressed, particle formation had a greater proportional effect on aerosol in 1850 than in 2000, and vice versa in regions where albedo changes are enhanced. A greater proportional effect in 1850 can be explained in two ways: that industrial emissions of precursor gases and primary aerosol in 2000 have acted to suppress particle formation, implying that increases in the condensation sink have outweighed increases in the nucleating H_2SO_4 vapour, or that a greater fraction of CDNC are due to primary particles in 2000.

4 Conclusions and discussion

We have used a global aerosol model to explore the consequences of boundary layer particle formation on global and regional CDNC. The obtained CDNC with particle formation are in good agreement with in-situ observations at marine and continental sites, while those without particle formation tend to underestimate CDNC. The effect on CDNC can be seen on most parts of the globe, but the relative contribution of particle

ACPD
9, 5263–5287, 2009

formation to regional CDNC varies greatly. Furthermore, this contribution is nonlinear to in-situ particle formation rates. Particle formation can greatly enhance CDNC also in regions where in-situ formation rates are negligible due to long range transport of aerosol.

Boundary layer particle formation is not included in current GCMs. However, our study suggests that particle formation could have significant consequences for the calculation of cloud albedo changes. Model simulations using emissions for 1850 and 2000 show that particle formation made a nearly equal contribution (16%–13.5%) to global CDNC in both years. However, there are distinct regional differences in the historical contribution of particle formation to CDNC that can affect albedo changes by more than 50%. We find that there is a strong North-South contrast in the obtained albedo changes due to particle formation. With some exceptions, particle formation decreases the albedo changes in the polluted regions of Northern Hemisphere and increases the albedo changes in the Southern Hemisphere. In the Arctic particle formation appears to suppress the 1850 to 2000 summertime albedo change by as much as 43%. Thus, particle formation was a much more important source of CDNC in the Arctic in 1850 than today. The explanation is that the sulfur pollution in the modern-day Arctic exists as a sulfate aerosol, which act as a sink for new particles, rather than SO_2, which would act as a source for particle formation.

These results should be considered as a first attempt to quantify the importance of boundary layer particle formation for long term changes in cloud drop number and albedo. Of importance for the pattern of radiative forcing is that particle formation enhances the long term increase in CDNC in the persistent stratocumulus regions to the west of Africa and west of South America. Without particle formation, the CDNC change west of South America is predicted to be 18.7% but with particle formation it is 29.0%. This leads to an estimated 49% enhancement in the 1850-to-2000 change in cloud albedo. New observations combined with high resolution cloud-scale modelling of outflow of pollutants from South America are needed to improve our low resolution model estimate. On the persistent stratocumulus region east of North-East Asia the

ACPD
9, 5263–5287, 2009

1850–2000 albedo enhancement is particularly strong. With particle formation, the obtained albedo enhancement is reduced by 18.4%.

The impact on climate change needs to be considered in longer simulations that include a calculation of cloud radiative forcing and the co-location of cloud type and CDNC change. Substantial changes in cloud albedo are predicted in regions with persistent low level clouds, but there are also substantial effects on CDNC in regions where other cloud types dominate. The substantial suppression of summertime Arctic indirect effect needs further investigation. Our model captures Arctic summertime particle size distribution fairly well (Korhonen et al., 2008) but, given the importance of Arctic climate change, further work is needed in this area. We also find that the effect of particle formation on CDNC becomes more pronounced at higher updraft velocities since smaller particles become activated. Climate model simulations of the effects of CDNC on high updraft cumulus clouds are at an early stage (Wu et al., 2007), but nucleation could have an important influence on long term changes in CDNC in these clouds.

There are also uncertainties in the particle formation rate that affect the results (Spracklen et al., 2008). The fundamental mechanism of particle formation is still poorly understood, and the process may be limited by the abundance of some other chemical species beside sulfuric acid as assumed here. For example, it has been suggested that the neutral activated cluster may constitute ammonia and sulfuric acid (Vehkamaki et al., 2004; Ortega et al., 2008), which may affect the nucleation rate in some regions (Gaydos et al., 2005; Jung et al., 2006). It has also been shown that biogenic organic species could control the nucleation rate (Bonn et al., 2008), which would lead to suppressed particle formation over marine regions. It may take time before the fundamental mechanism, or mechanisms, of atmospheric particle formation are resolved. However, since its contribution to CDNC and total particle concentrations appears to be large, best available representations should be utilized when estimating of the effects of aerosols on climate.

ACPD
9, 5263–5287, 2009

Acknowledgements. This work was supported by grants from NERC (AEROFORM NE/D01395X/1 and APPRAISE theme 3), a Royal Society International Joint Project, and the EU EUCAARI integrated project. J. Merikanto was also supported by Academy of Finland grant no. 126105.

References

Adams, P. J. and Seinfeld, J. H.: Predicting global aerosol size distributions in general circulation models, J. Geophys. Res., 107(D19), 4370, doi:10.1029/2001JD001010, 2002. 5265

Bond, T., Bhardwaj, E., Dong, R., Jogani, R., Jung, S., Roden, C., Streets, D. G., and Trautmann, N. M.: Historical emissions of black and organic carbon aerosol from energy-related combustion, 1850–2000, Global Biogeochem. Cycles, 21, GB2018, doi:10.1029/2006GB002840, 2007. 5268

Bonn, B., Kulmala, M., Riipinen, I., Sihto, S.-L., and Ruuskanen, T. M.: How biogenic terpenes govern the correlation between sulfuric acid concentrations and new particle formation, J. Geophys. Res., 113, D12209, doi:10.1029/2007JD009327, 2008. 5275

Chipperfield, M.: New version of the TOMCAT/SLIMCAT off-line chemical transport model: Intercomparison of stratospheric tracer experiments, Q. J. R. Meteorol. Soc., 132, 1179–1203, doi:10.1256/qj.05.51, 2006. 5266

Dentener, F., Kinne, S., Bond, T., Boucher, O., Cofala, J., Generoso, S., Ginoux, P., Gong, S., Hoelzemann, J. J., Ito, A., Marelli, L., Penner, J. E., Putaud, J.-P., Textor, C., Schulz, M., van der Werf, G. R., and Wilson, J.: Emissions of primary aerosol and precursor gases in the years 2000 and 1750 prescribed data-sets for AeroCom, Atmos. Chem. Phys., 6, 4321–4344, 2006, http://www.atmos-chem-phys.net/6/4321/2006/. 5268

Dusek, U., Frank, G. P., Hildebrandt, L., Curtius, J., Schneider, J., Walter, S., Chand, D., Drewnick, F., Hings, S., Jung, D., Borrmann, S., and Andreae, M. O.: Size Matters More Than Chemistry for Cloud-Nucleating Ability of Aerosol Particles, Science, 312, 1375, doi:10.1126/science.1125261, 2006. 5264

Fernandes, S. D., Trautmann, N. M., Streets, D. G., Roden C. A., and Bond, T. C.: Global biofuel use, Global Biogeochem. Cycles, 21, GB2019, doi:10.1029/2006GB002836, 2007. 5268

Fountoukis, C. and Nenes, A.: Continued developement of a cloud droplet formation

parameterization for global climate models, J. Geophys. Res.–Atmos., 110, D11212, doi:10.1029/2004JD005591, 2005. 5268
Fountoukis, C., Nenes, A., Meskhidze, N., Bahreini, R., Conant, W. C., Jonsson, H. Murphy, S., Sorooshian, A., Varutbangkul, V., Brechtel, F., Flagan, R. C., and Seinfeld, J. H.: Aerosol-cloud drop concentration closure for clouds sampled during the International Consortium for Atmospheric Research on Transport and Transformation 2004 campaign, J. Geophys. Res., 112, D10S30, doi:10.1029/2006JD007272, 2007. 5269, 5281
Gaydos, T. M., Stanier, C. O., and Pandis, S. N.: Modeling of in situ ultrafine atmospheric particle formation in the eastern United States, J. Geophys. Res., 110, D07S12, doi:10.1029/2004JD004683, 2005. 5266, 5275
Gong, S. L.: A parameterization of sea-salt aerosol source function for sub- and super-micron particles, Global Biogeochem. Cycles, 17(4), 1097, doi:10.1029/2003GB002079, 2003. 5269
Guenther, A., Hewitt, C. N., and Erickson, D., et al.: A global model of natural volatile organic compound emissions, J. Geophys. Res., 100, 8873–8892, doi:10.1029/94JD02950, 1995. 5266
Gultepe, I. and Isaac, G. A.: The effects of air-mass origin on Arctic cloud microphysical parameters during FIRE.ACE, J. Geophys. Res., 107(C10), 8029, doi:10.1029/2000JC000440, 2002. 5269, 5281
Gultepe, I. and Isaac, G. A.: Aircraft observations of cloud droplet number concentration: Implications for climate studies, Q. J. R. Meteorol. Soc., 130, 2377-2390, 2004. 5269, 5281
Hirsikko, A., Laakso, L., Horrak, U., Aalto, P. P., Kerminen, V. M., and Kulmala, M.: Annual and size dependent variation of growth rates and ion concentrations in boreal forest, Boreal Environ. Res., 10(5), 357–369, 2005. 5267
IPCC: 4th Assessment Report of the Intergovernmental Panel on Climate Change, IPCC, Geneva, Switzerland, WG1, 502, 2007. 5264
Jung, J., Adams, P. J., and Pandis, S. N.: Simulating the size distribution and chemical composition of ultrafine particles during nucleation events, Atmos. Environ., 40, 2248–2259, 2006. 5266, 5275
Kerminen, V.-M. and Kulmala, M.: Analytical formulae connecting the “real” and the apparent nucleation rate and the nuclei number concentration for atmospheric nucleation events, J. Aerosol Sci., 33, 609–622, 2002. 5267
Kerminen, V.-M., Lihavainen, H., Komppula, M., Viisanen, Y., and Kulmala, M.: Direct observational evidence linking atmospheric aerosol formation and cloud droplet activation, Geophys.

Res. Lett., 32, L14803, doi:10.1029/2005GL023130, 2005. 5265
Korhonen, H., Carslaw, K. S., Spracklen, D. V., Ridley, D. A., and Ström, J.: A global model study of processes controlling aerosol size distribution in the Arctic spring and summer, J. Geophys. Res., 113, D08211, doi:10.1029/2007JD009114, 2008. 5275
Kuang, C., McMurry, P. H., McCormick, A. V., and Eisele, F. L.: Dependence of nucleation rates on sulfuric acid vapor concentration in diverse atmospheric locations, J. Geophys. Res., 113, D10209, doi:10.1029/2007JD009253, 2008. 5265
Kulmala, M., Laaksonen, A., and Pirjola, L.: Parameterizations for sulfuric acid/water nucleation rates, J. Geophys. Res.-Atmos., 103(D7), 8301–8307, 1998. 5265, 5267, 5268
Kulmala, M., Vehkamäki, H., and Petäjä, T., et al.: Formation and growth of ultrafine atmospheric particles: a review of observations, J. Aerosol Sci., 35, 143–176, doi:10.1016/j.jaerosci.2003.10.003, 2004a. 5265
Kulmala, M., Kerminen, V.-M., Anttila, T., et al.: Organic aerosol formation via sulfate cluster activation, J. Geophys. Res.-Atmos., 109(D4), D04205, doi:10.1029/2003JD003961, 2004b. 5267
Kulmala, M., et al. Lehtinen, K. E. J., and Laaksonen, A.: Cluster activation theory as an explanation of the linear dependence between formation rate of 3 nm particles and sulfuric acid concentration, Atmos. Chem. Phys., 6, 787–793, 2006, http://www.atmos-chem-phys.net/6/787/2006/. 5267
Laaksonen, A., Hamed, A., Joutsensaari, J., Hiltunen, L., Cavalli, F., Junkermann, W., Asmi, A., Fuzzi, S., and Facchini, M. C.: Cloud condensation nucleus production from nucleation events at a highly polluted region, Geophys. Res. Lett., 32, L06812, doi:10.1029/2004GL022092, 2005. 5265
Lihavainen, H., Kerminen, V.-M., Komppula, M., Hatakka, J., Aaltonen, V., Kulmala, M., and Viisanen, Y.: Production of "potential" cloud condensation nuclei associated with atmospheric new-particle formation in northern Finland, J. Geophys. Res., 108(D24), 4782, doi:10.1029/2003JD003887, 2005. 5265
Lohmann, U. and Feichter, J.: Global indirect aerosol effects: a review, Atmos. Chem. Phys., 5, 715–737, 2005, http://www.atmos-chem-phys.net/5/715/2005/. 5264
Merikanto, J., Napari, I., Vehkamäki, H., Anttila, T., and Kulmala, M.: New parameterization of ternary sulfuric acid-ammonia-water ternary nucleation rates at tropospheric conditions, J. Geophys. Res.-Atmos., 112, D15207, doi:10.1029/2006JD007977, 2007. 5267

Meskhidze, N., Nenes, A., Conant, W. C., and Seinfeld, J. H.: Evaluation of a new cloud droplet activation parameterization with in situ data from CRYSTAL-FACE and CSTRIPE, J. Geophys. Res., 110, D16202, doi:10.1029/2004JD005703, 2005. 5268, 5269, 5281

Nenes, A. and Seinfeld, J. H.: Parameterization of cloud droplet formation in global climate models, J. Geophys. Res.-Atmos., 108(D14), 4415, doi:10.1029/2002JD002911, 2003. 5264, 5268

O'Dowd, C. D., Aalto, P., Hämeri, K., Kulmala, M., and Hoffmann, T.: Atmospheric particles from organic Vapours, Nature, 416, 497–498, 2002a. 5265

Ortega, I. K., Kurtén, T., Vehkamäki, H., and Kulmala, M.: The role of ammonia in sulfuric acid ion induced nucleation, Atmos. Chem. Phys., 8, 2859–2867, 2008, http://www.atmos-chem-phys.net/8/2859/2008/. 5275

Penner, J. E., Quaas, J., Storelvmo, T., Takemura, T., Boucher, O., Guo, H., Kirkevôg, A., Kristjánsson, J. E., and Seland, Ø.: Model intercomparison of indirect aerosol effects, Atmos. Chem. Phys., 6, 3391–3405, 2006, http://www.atmos-chem-phys.net/6/3391/2006/. 5265

Riipinen, I., Sihto, S.-L., Kulmala, M., Arnold, F., Dal Maso, M., Birmili, W., Saarnio, K., Teinilä, K., Kerminen, V.-M., Laaksonen, A., and Lehtinen, K. E. J.: Connections between atmospheric sulphuric acid and new particle formation during QUEST III/IV campaigns in Heidelberg and Hyytiälä, Atmos. Chem. Phys., 7, 1899–1914, 2007, http://www.atmos-chem-phys.net/7/1899/2007/. 5265

Schroder F. P., Karcher, B., Fiebig, M., and Petzold, A.: Aerosol states in the free troposphere at northern midlatitudes, J. Geophys. Res., 107(D21), 8126, doi:10.1029/2000JD000194, 2002. 5267

Smith, S. J., Andres, R., Conception, E., and Lurz, J.: Historical sulfur dioxide emissions: Methods and results, PNNL Research Report, PNNL-14537, 1850–2000, 2004. 5268

Sihto, S.-L., Kulmala, M., Kerminen, V.-M., Dal Maso, M., Petäjä, T., Riipinen, I., Korhonen, H., Arnold, F., Janson, R., Boy, M., Laaksonen, A., and Lehtinen, K. E. J.: Atmospheric sulphuric acid and aerosol formation: implications from atmospheric measurements for nucleation and early growth mechanisms, Atmos. Chem. Phys., 6, 4079–4091, 2006, http://www.atmos-chem-phys.net/6/4079/2006/. 5265, 5267

Spracklen, D. V., Pringle, K. J., Carslaw, K. S., Chipperfield, M. P., and Mann, G. W.: A global off-line model of size-resolved aerosol microphysics: I. Model development and prediction of aerosol properties, Atmos. Chem. Phys., 5, 2227–2252, 2005,

http://www.atmos-chem-phys.net/5/2227/2005/. 5265, 5266, 5268
Spracklen, D. V., Carslaw, K. S., Kulmala, M., Kerminen, V.-M., Mann, G. W., and Sihto, S.-L.: The contribution of boundary layer nucleation events to total particle concentrations on regional and global scales, Atmos. Chem. Phys., 6, 5631–5648, 2006, http://www.atmos-chem-phys.net/6/5631/2006/. 5265, 5267
Spracklen, D.,Carslaw, K. S., Kulmala, M., Kerminen, V.-M., Sihto, S.-L., Riipinen, I., Merikanto, J., Mann, G. W., Chipperfield, M. P., Wiedensohler, A., Birmili, W., and Lihavainen, H.: Contribution of particle formation to global condensation nuclei concentrations, Geophys. Res. Lett., 35, L06808, doi:10.1029/2007GL033038, 2008. 5265, 5267, 5275
Twomey, S.: Aerosols, clouds and radiation, Atmos. Environ. A-Gen, 25, 2435–2442, 1991. 5264, 5271
Vehkamäki, H., Napari, I., Kulmala, M., and Noppel, M.: Stable ammonium bisulphate clusters in the atmosphere, Phys. Rev. Lett., 93, 148501, doi:10.1103/PhysRevLett.93.14850, 2004. 5275
Weber, R. J., McMurry, P. H., Eisele, F. L., and Tanner, D. J.: Measurements of expected nucleation precursor species and 3–500 nm diameter particles at Mauna Loa observatory, Hawaii, J. Atmos. Sci., 52, 2242–2257, 1995. 5265
Weber, R. J., McMurry, P. H., Eisele, F. L., Tanner, D. J., and Jefferson, A.: Measurements of new particle formation and ultrafine particle growth rates at a clean continental site, J. Geophys. Res., 102, 4375–4385, 1997. 5265
Wu, J., Zhang, M., and Lin, W.: A case study of a frontal system simulated by a climate model: Clouds and radiation, J. Geophys. Res., 112, D12201, doi:10.1029/2006JD008238, 2007. 5275

Table 1. Comparison of modelled 2000 CDNC [cm^3] to CDND observed in in-situ measurement campaigs. Model calculations are carried out with typical updraught velocities ($\overline{w}$) observed during the campaigns. Results are shown with (BLPF) and without (no BLPF) boundary layer particle formation.

Location	$\overline{w}$	no BLPF	BLPF	Obs.
Beaufort sea (April)	0.4	70	86	90[1]
Key West (July)	2.0	409	631	836±727[2]
Monterey (July)	0.2	274	298	378±72[2]
Cleveland (August)	0.4	566	763	881±285[3]

[1] Gultepe and Isaac (2002, 2004)
[2] Meskhidze et al. (2005)
[3] Fountoukis et al. (2007)

ACPD
9, 5263–5287, 2009

Table 2. Summary of yearly average CDNC [cm^{-3}] and ΔRc obtained from model runs. Primed values indicate results without BLPF. CDNC is calculated with an updraft velocity $\overline{w}$=0.4 m/s. ΔRc is the coresponding change in albedo for an initial albedo of Rc=0.35. The last column shows the correction from BLPF to albedo change, $(\Delta Rc - \Delta Rc')/\Delta Rc'$. The marine regions refer to west of North America (NAM), west of South America (SAM), west of North Africa (NAF), west of South Africa (SAF), and east of North-East Asia (NEA) (see Fig. 2).

	1850		2000				
Region	CDNC′	CDNC	CDNC′	CDNC	ΔRc′%	ΔRc%	$\frac{d\Delta Rc}{\lvert\Delta Rc'\rvert}$%
Total Global	125	145	211	240	3.97	3.85	−3.0
Arctic	54	81	86	116	3.60	2.72	−24.3
North temperate zone	139	173	325	374	6.47	5.85	−9.6
Northern tropics	141	161	250	274	4.33	4.03	−6.7
Southern tropics	167	178	217	243	1.97	2.35	19.4
South temperate zone	88	101	104	125	1.30	1.64	25.8
Antarctic	56	64	56	64	0.027	0.053	94.5
Total Marine	102	117	155	176	3.13	3.09	−1.2
NAM	99	114	214	236	5.81	5.52	−5.0
SAM	107	116	127	149	1.30	1.94	49.2
NAF	92	113	199	241	5.82	5.76	−0.9
SAF	142	151	165	186	1.17	1.58	34.7
NEA	127	168	352	389	7.77	6.34	−18.4
Total Continental	186	219	362	413	5.04	4.81	−4.7
Europe	232	291	562	621	6.73	5.75	−14.6
Africa	233	263	377	419	3.65	3.52	−3.6
N. America	170	215	330	419	5.05	5.05	0.1
S. America	250	274	408	466	3.72	4.02	8.1
N. Asia	117	152	280	336	6.63	6.00	−9.5
SE Asia	203	245	558	598	7.65	6.75	−11.8
Oceania	219	243	287	352	2.05	2.80	36.1

ACPD
9, 5263–5287, 2009

,

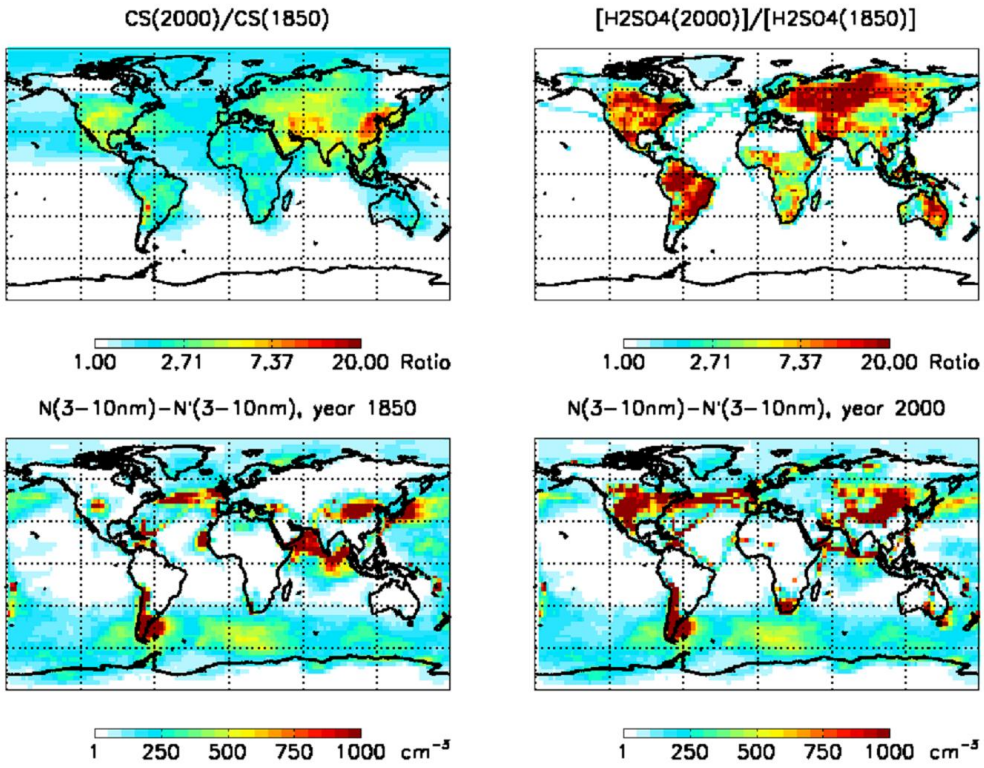

Fig. 1. Upper panels: The ratio of annual mean 2000 and 1850 values for condensation sink (CS) and gas-phase sulfuric acid concentration. Lower panels: The difference in concentrations of 3–10 nm particles with (N) and without (N') boundary layer particle formation in 1850 and 2000.

ACPD
9, 5263–5287, 2009

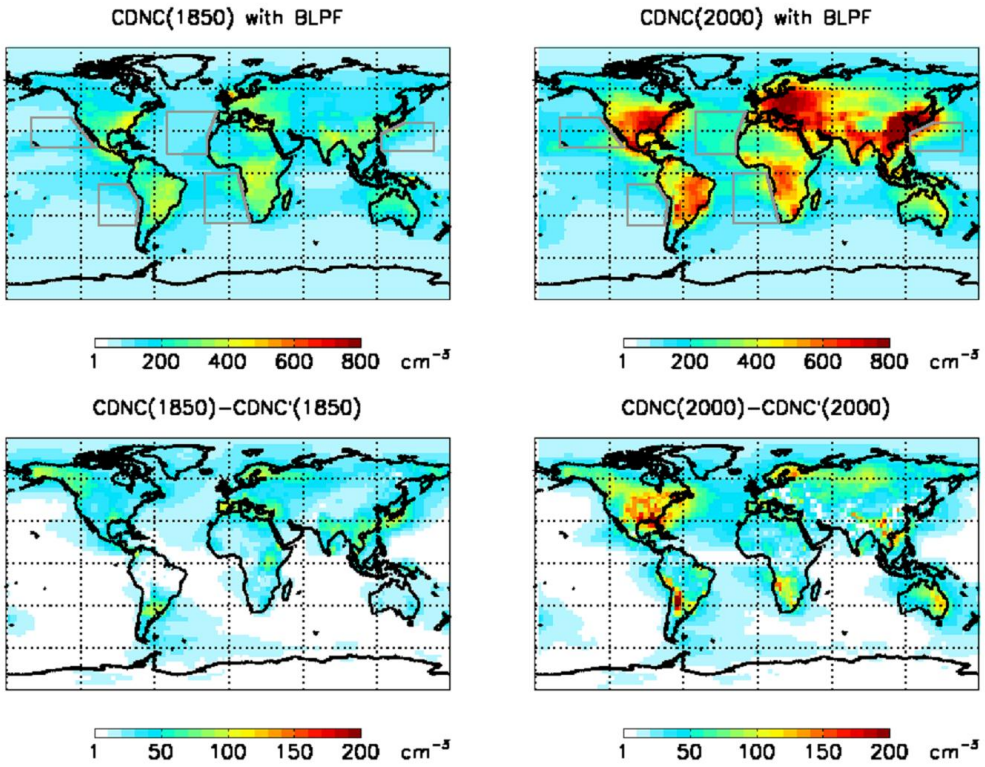

Fig. 2. Upper panels: Annual mean cloud droplet number concentration with BL particle formation on 1850 and 2000. Lower panels: The difference in cloud droplet number concentration with and without BL particle formation in 1850 and 2000. The updraft velocity is taken to be $\overline{w}$=0.4m/s in all cases.

ACPD
9, 5263–5287, 2009

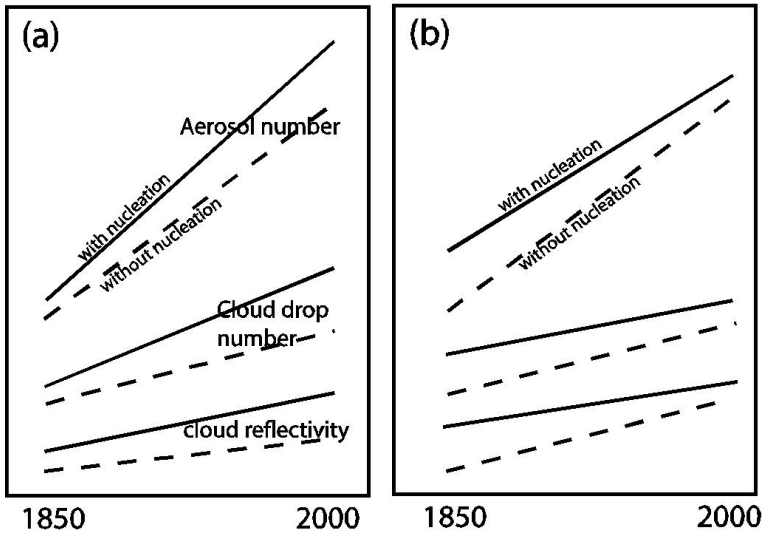

Fig. 3. Schematic showing how the inclusion of boundary layer nucleation can either increase or decrease the change in cloud albedo (ΔRc) between 1850 and 2000. **(a)** Nucleation increases ΔRc: the fractional impact of nucleation on aerosol number, cloud drop number and cloud albedo is less in 1850 than in 2000. **(b)** Nucleation decreases ΔRc: the fractional impact of nucleation on aerosol number, cloud drop number and cloud albedo is greater in 1850 than in 2000. Note that fractional changes in CDNC are always smaller than fractional changes in aerosol number, and fractional changes in Rc are smaller still. So although the change in aerosol between 1850 and 2000 is much larger than any effect of particle formation, this is not the case for changes in albedo. The effect is exaggerated in the diagram.

ACPD
9, 5263–5287, 2009

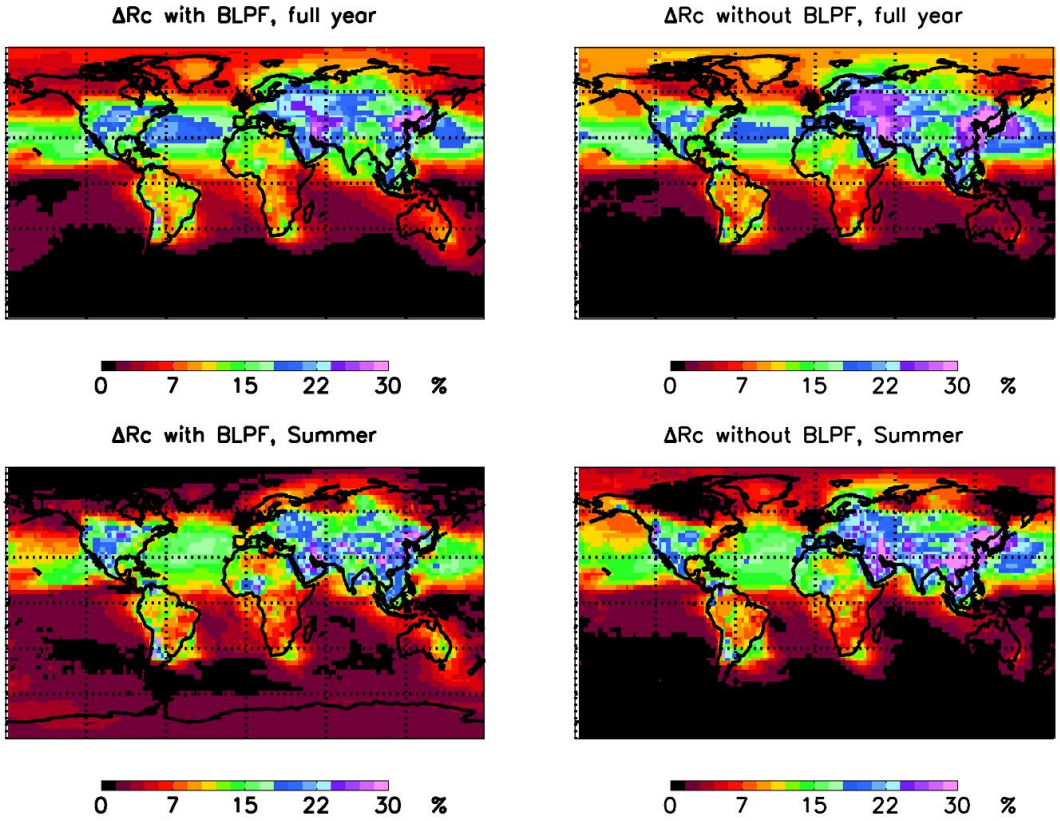

Fig. 4. The change in cloud albedo with and without boundary layer particle formation. Results are shown for an initial albedo Rc=0.35 assuming cloud updraft velocity $\overline{w}$=0.4m/s.

ACPD
9, 5263–5287, 2009

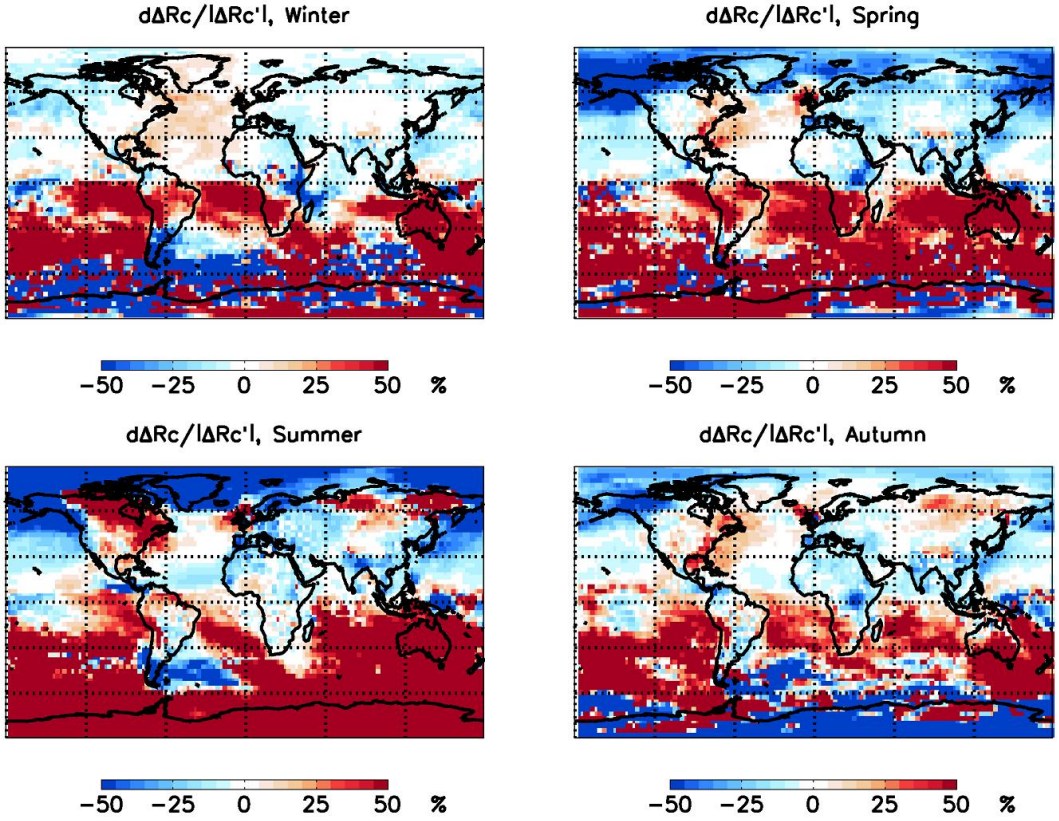

Fig. 5. Upper panel: The relative error in calculation of the albedo change if particle formation is neglected. Results are shown for four Northern Hemisphere seasons. The updraft velocity is taken to be $\overline{w}$=0.4m/s.

ACPD
9, 5263–5287, 2009